Supplemental information

Anti-Poisoning of CO and Carbonyl Species over Pd Catalysts During the Electrooxidation of Ethylene Glycol to Glycolic Acid at Elevated Current Density

Jia Cheng, Yunchuan Tu, Yang Xiang, Jingtian Ni, Tao Guo, Xun Huang[a], Bin Liu*[b], Zidong Wei*[a]*

[a]Center of Advanced Electrochemical Energy, State Key Laboratory of Advanced Chemical Power Sources, School of Chemistry and Chemical Engineering, Chongqing University, Chongqing 40004, China

[b]Department of Materials Science and Engineering, City University of Hong Kong, Hong Kong, 999077, China

*Corresponding author e-mail: huangxun@cqu.edu.cn (X. H.), bliu48@cityu.edu.hk, and zdwei@cqu.edu.cn (Z.W.)

Experimental Section

Chemicals and materials

$PdCl_2$ (99.5%) was obtained from Shanghai Jiuyue Chemical Co. All chemicals used were of analytical grade and not further purified.

Synthesis of PdM/C

Vulcan XC 72R (40 mg) was dispersed in 40 mL ethylene glycol and sonicated for 1 h until the carbon was fully dispersed at room temperature. Next, 500 μL K_2PdCl_4 (5 mM), 200 μL $NiCl_2$ (5 mM) and 200 μL Na_2MoO_4 (5 mM) in an EG solution were added to the mixture. The pH was then adjusted to 10 by adding a solution of NaOH in ethylene glycol, followed by magnetic stirring for 20 min. The solution obtained was transferred into a round-bottomed flask and then subjected to reflux through condensation at 160°C for 6 h. After natural cooling and filtration, the synthesized products were washed three times with acetone, ethanol, and deionized (DI) water, respectively. Afterward, the PdNiMo/C catalyst was collected by drying it overnight at 60°C under vacuum. Different Pd-based catalytic materials can be produced by adjusting the content and type of precursors in the reaction mixture, including Pd/C, PdNi/C, and PdMo/C.

Structural Characterization

The microstructure and morphology of the prepared catalysts were analyzed using X-ray diffraction (XRD-6000, Shimadzu) and transmission electron microscopy (Talos F200S). The elemental composition, valence, and distribution of the catalysts were determined through X-ray photoelectron spectroscopy (ESCALAB250XI) and inductively coupled plasma emission spectrometry (iCAP 6300 Duo).

Electrochemical Measurements

Electrochemical measurements were conducted using a CHI 660e electrochemical workstation throughout the experiments. An H-type electrolyzer was used, with carbon paper (1 cm × 1 cm) coated with catalyst as the working electrode, Hg/HgO electrode as the reference electrode and graphite sheet electrode as the counter electrode. Unless otherwise stated, all potentials mentioned herein have been converted to the relative reversible hydrogen electrode (RHE) scale using the following equation:

$$E_{RHE} = E_{Hg/HgO} + 0.2412\ V + 0.059\ pH \qquad (1)$$

Preparation of electrode materials: 2 mg of the prepared powder catalyst was weighed and dispersed by adding 400 μL of isopropanol and 10 μL of Nafion and then sonicated for 30 min. After ultrasonic homogenization, it was drop coated on the surface of carbon paper and used as a working electrode.

During the testing, a water bath was used to keep the reaction temperature at 25°C and nitrogen (N_2) was continuously circulated through the reaction to remove dissolved oxygen from the solution.

Product Analysis

After electrolysis, the electrolyte was neutralized by a cation exchange resin before being passed through a liquid chromatography column (Aminex HPX-87H Column) for product analysis. The Faraday efficiency (FE) of the electrolytic oxidation products was calculated as follows:

$$FE_i = \frac{\sum n_i Z_i F}{Q} \qquad (2)$$

where n_i is the moles of oxidation product i, Z_i is the number of transferred electrons to form compound i, F is the Faraday constant (96485.3 C mol^{-1}), and Q is the actual Coulombs consumed during electrolysis.

Electrochemical *in-situ* infrared test methods

A gold-plated semicircular silicon prism served as the working electrode, and a FTIR spectrometer (Bruker, Vertex 70V) with an attenuated total reflection-surface enhanced infrared absorption spectroscopy (ATR-SEIRAS) configuration was used to detect adsorbed species on Au films. The catalyst ink prepared above was drop-coated 20 μL on the electroplated monocrystalline silicon surface. The catalytic material was activated in 1.0 M KOH electrolyte and later transferred to a solution containing 1.0 M

EG for *in-situ* IR testing. Scanning potentials were varied from 0 V vs. RHE to 1.4 V vs. RHE.

Theoretical Calculation Methods

All calculations in this work are conducted using first-principles density-functional theory (DFT) with the Vienna Ab initio Simulation Package (VASP). The projector augmented wave (PAW) pseudopotential was utilized to represent the core electrons, with a cutoff energy of 500 eV for the plane wave basis set describing the valence electrons. The exchange correlation function was determined using the generalized gradient approximation (GGA) proposed by Perdew-Burke-Ernzerhof (PBE), and the electron occupancy was determined using a Gaussian method with a smearing width of 0.05 eV.

The Pd (1 1 1) surface was constructed using a p (4 × 4) supercell containing four layers (16 atoms per layer) with a 15 Å vacuum. By randomizing the doping of Ni and Mo atoms within the established Pd (1 1 1) layer, it is ensured that the position of the doping remains constant each time. A 3 × 3 × 1 k-point grid using the Monkhorst-Pack method was selected. The calculations enable the top two layers of metals to relax, while the bottom two layers remain fixed in their optimized bulk lattice positions. The adsorption energy of species A on catalyst B surface is calculated using the following equation:[1, 2]

$$\Delta E_{ads} = E_{A/B} - E_A - E_B$$

(3)

where $E_{A/B}$, E_A and E_B denote the total energy of A adsorbed on B, the separated species A and catalyst B, respectively.

The Gibbs free energy (ΔG) of the EGOR reaction process was calculated based on the computational hydrogen electrode (CHE) model proposed by Nørskov et al.[3, 4] At 298.15 K, 0.035 bar of air pressure, the free energies of liquid and gaseous H_2O are comparable, thus $G_{H_2O(l)} = G_{H_2O(g)}$. At pH = 0, $G(H^+ + e^-) = \frac{1}{2}G(H_2)$. The free energy change for each step of the reaction is calculated as follows:

$$\Delta G = \Delta E + \Delta ZPE + \Delta TS \qquad (4)$$

where ΔE is the energy difference between the reactants and products calculated by DFT. ZPE and TS are the corrections to the zero-point energy and entropy, respectively, both obtained from frequency calculation.

Results and Discussion

Figure S1. Inductively coupled plasma optical emission spectroscopy (ICP-OES) test data of Pd/C, PdNi/C, PdMo/C, and PdNiMo/C

	Pd Load (%)	Ni Load (%)	Mo Load (%)	Ni/Pd	Mo/Pd
Pd/C	7.83	0.00	0.00	0.00	0.00
PdNi/C	2.70	0.52	0.00	0.19	0.00
PdMo/C	3.73	0.00	0.18	0.00	0.06
PdNiMo/C	1.83	0.39	0.18	0.21	0.10

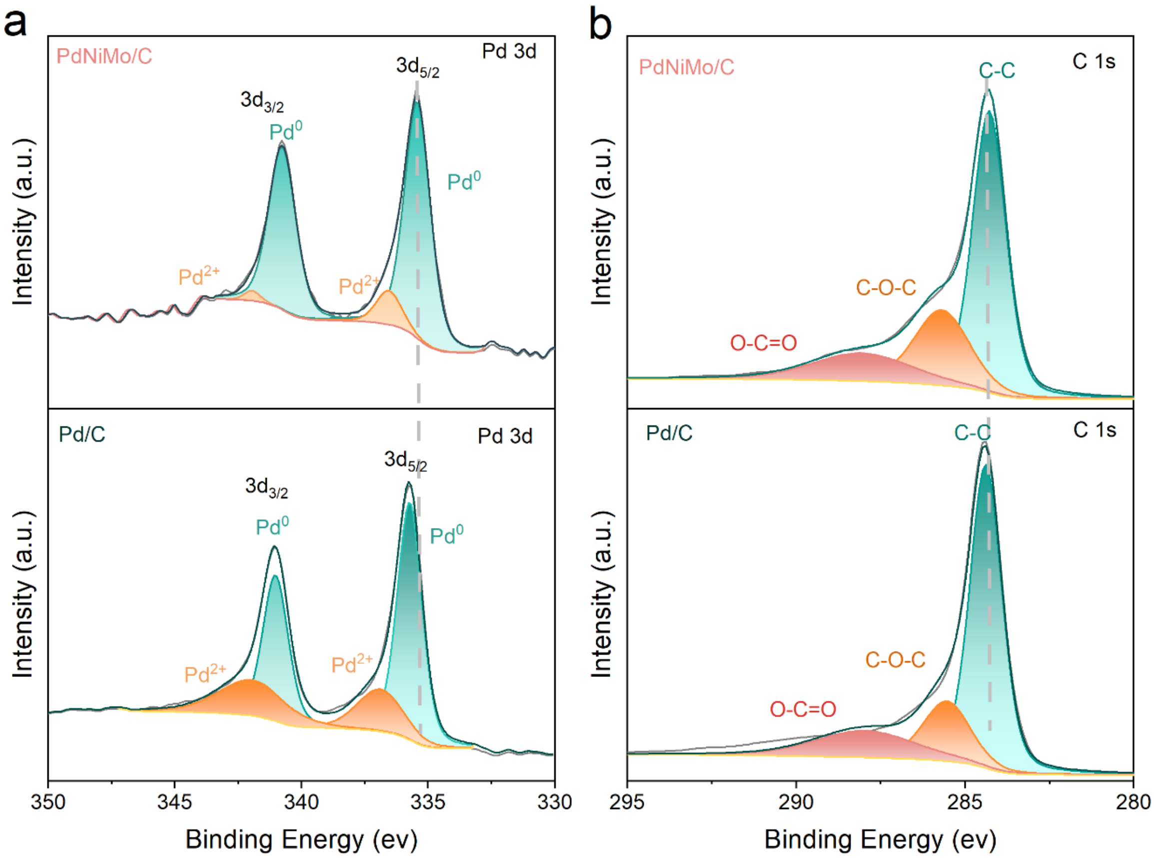

Figure S2. a) Pd 3d and b) C 1s XPS spectra of PdNiMo/C and Pd/C.

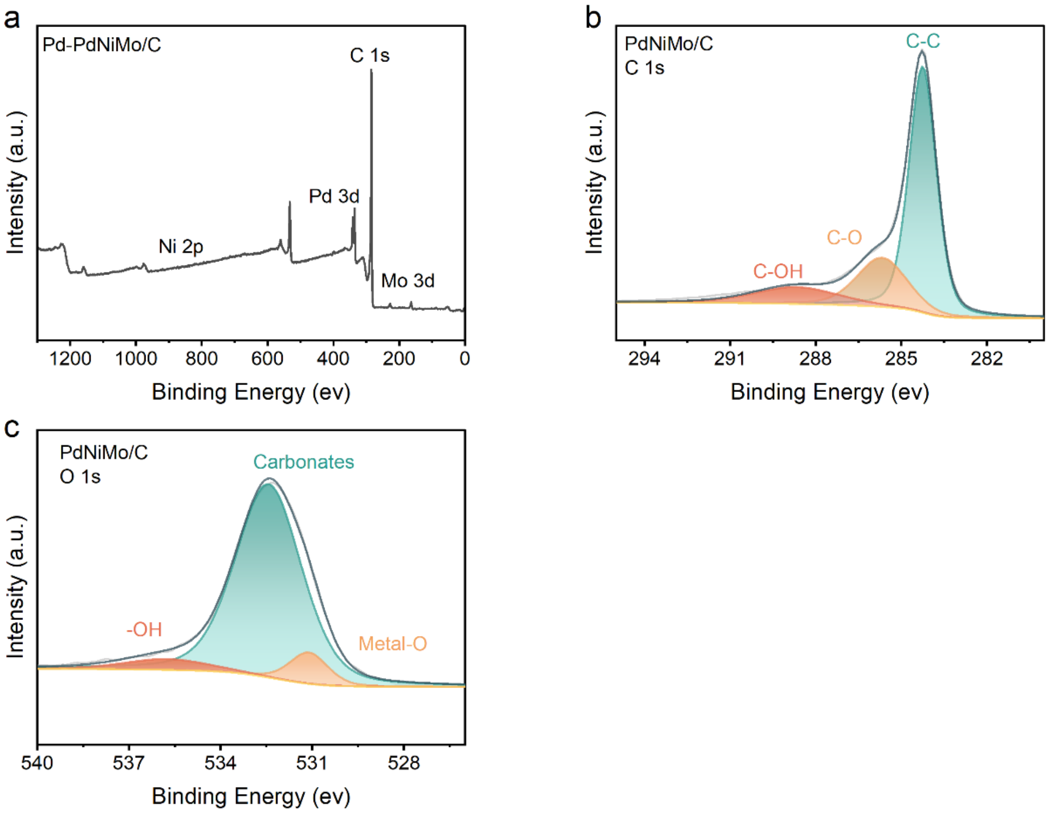

Figure S3. a) XPS survey spectra and XPS spectra of b) C 1s and c) O 1s in PdNiMo/C.

The measured element O comes mainly from oxygen in the air attached to the surface of the catalytic material.

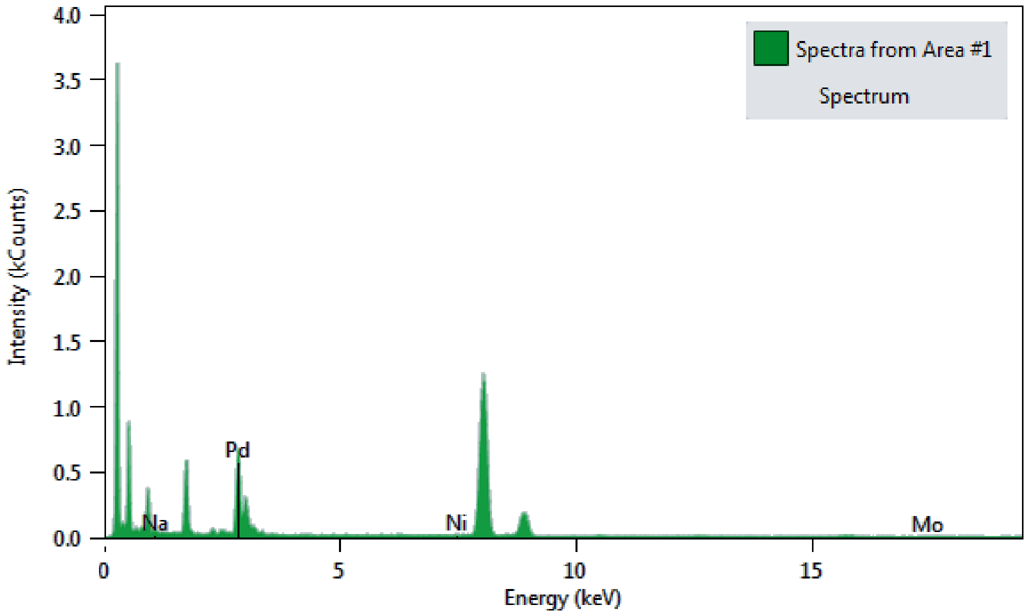

Figure S4. Energy dispersive spectroscopy (EDS) of PdNiMo/C.

Z	Element	Atomic Fraction (%)	Atomic Error (%)	Mass Fraction (%)	Mass Error (%)	Fit error (%)
28	Ni	16.59	0.65	9.97	0.28	5.96
42	Mo	8.13	0.32	7.99	0.25	14.20
46	Pd	75.28	21.37	82.04	15.77	0.18

The EDS elemental composition is basically consistent with the ICP test results, and it can be assumed that the elements in the catalyst are uniformly distributed, which is consistent with the TEM test results.

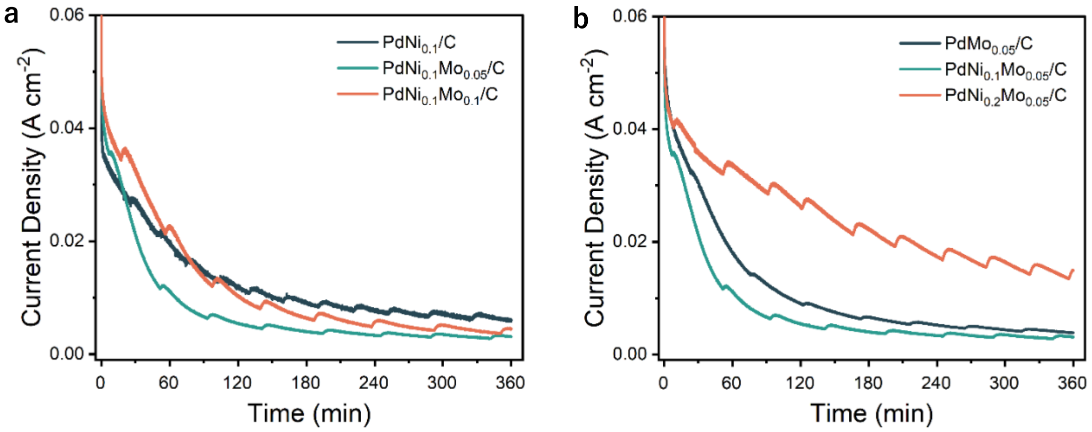

Figure S5. EGOR currents recorded over time on PdNiMo/C catalysts with different alloy ratios in 1.0 M EG + 1.0 M NaOH solution at 0.83 V vs. RHE.

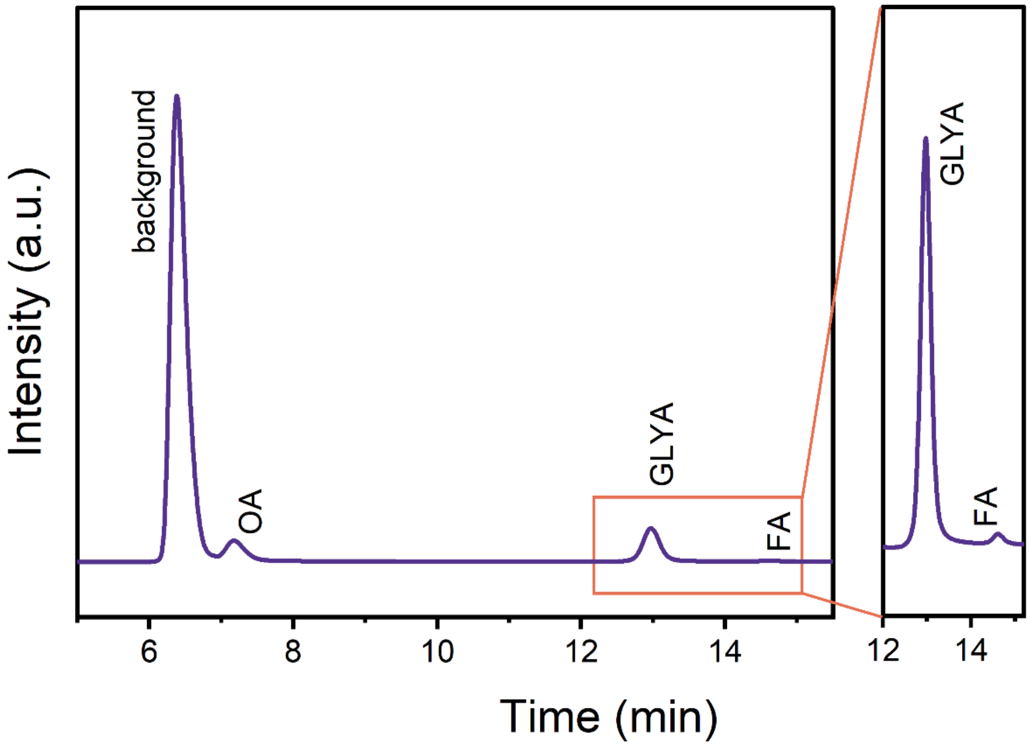

Figure S6. HPLC spectrum of the electrolyte after 6h of PdNiMo/C catalysis EG oxidation.

The background peaks in the HPLC spectrum are mainly generated from the electrolyte and exchanged with resin. The HPLC test detector is a UV absorption detector. Since the UV absorption of OA is stronger, the signal response is higher in the spectrum, but the overall concentration is lower.

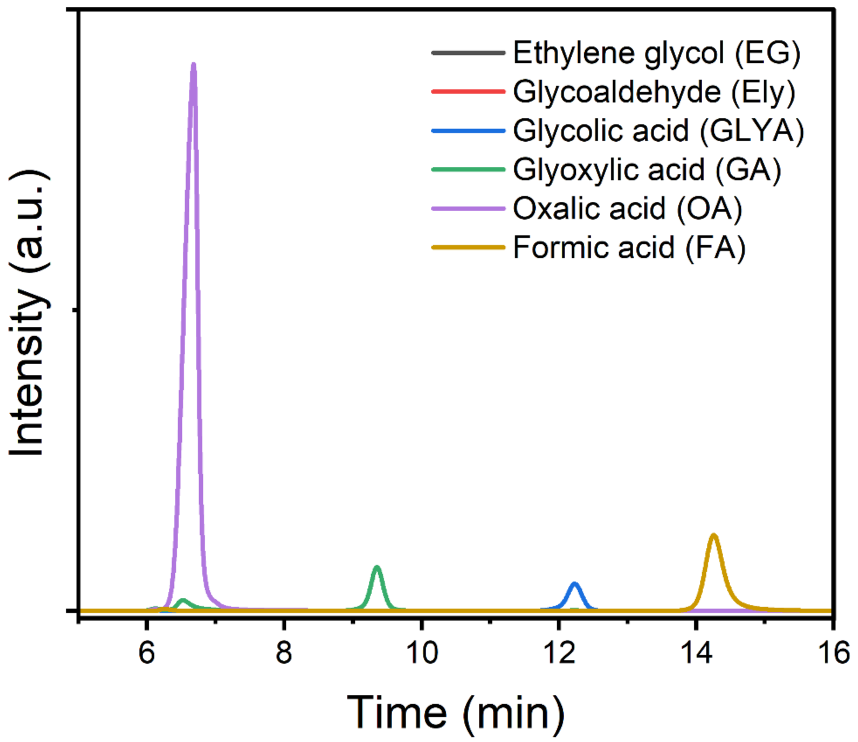

Figure S7. HPLC spectra of standard samples

HPLC test condition:

0.008 M sulfuric acid aqueous solution was selected as the mobile phase. The wavelength was 210nm. The flow rate was 0.6 ml/min, and the column temperature was controlled at 35°C.

Retention time of different oxidation products

	EG	Ely	GLYA	GA	OA	FA
retention time (min)	none	none	12.9	9.5	6.9	14.6

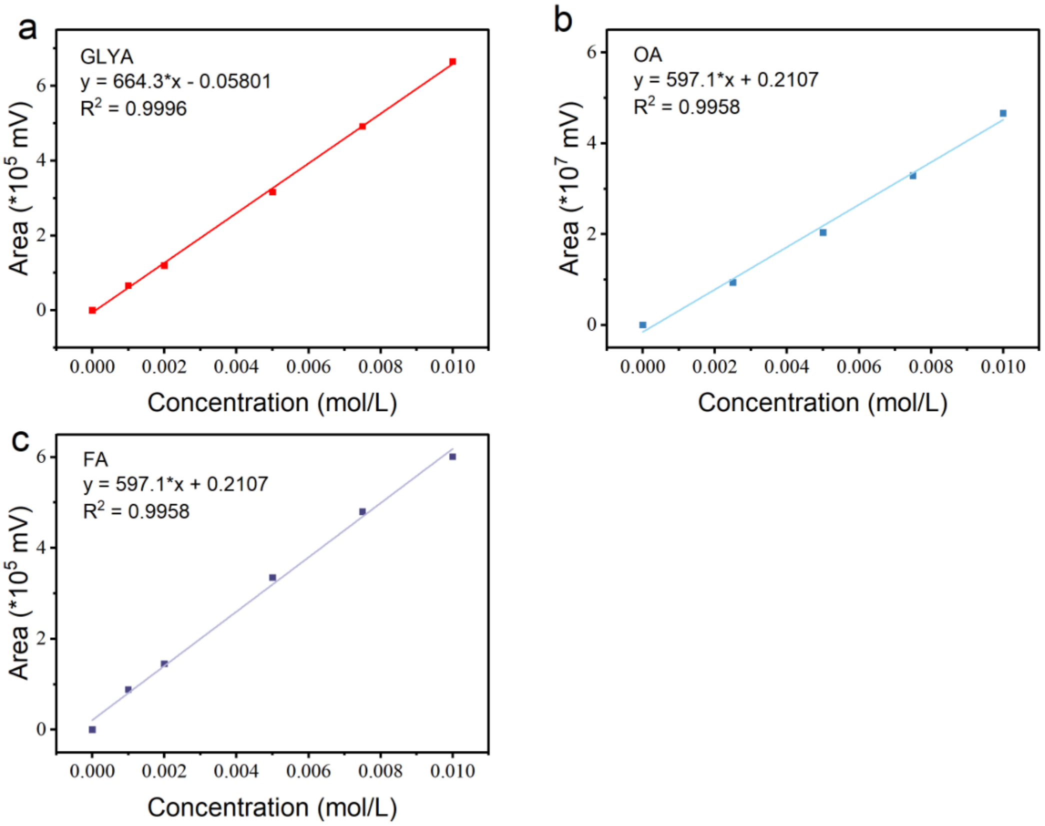

Figure S8. HPLC standard curve spectra of a) GLYA, b) OA, and c) FA.

The experimental data were averaged over three tests to minimize experimental errors.

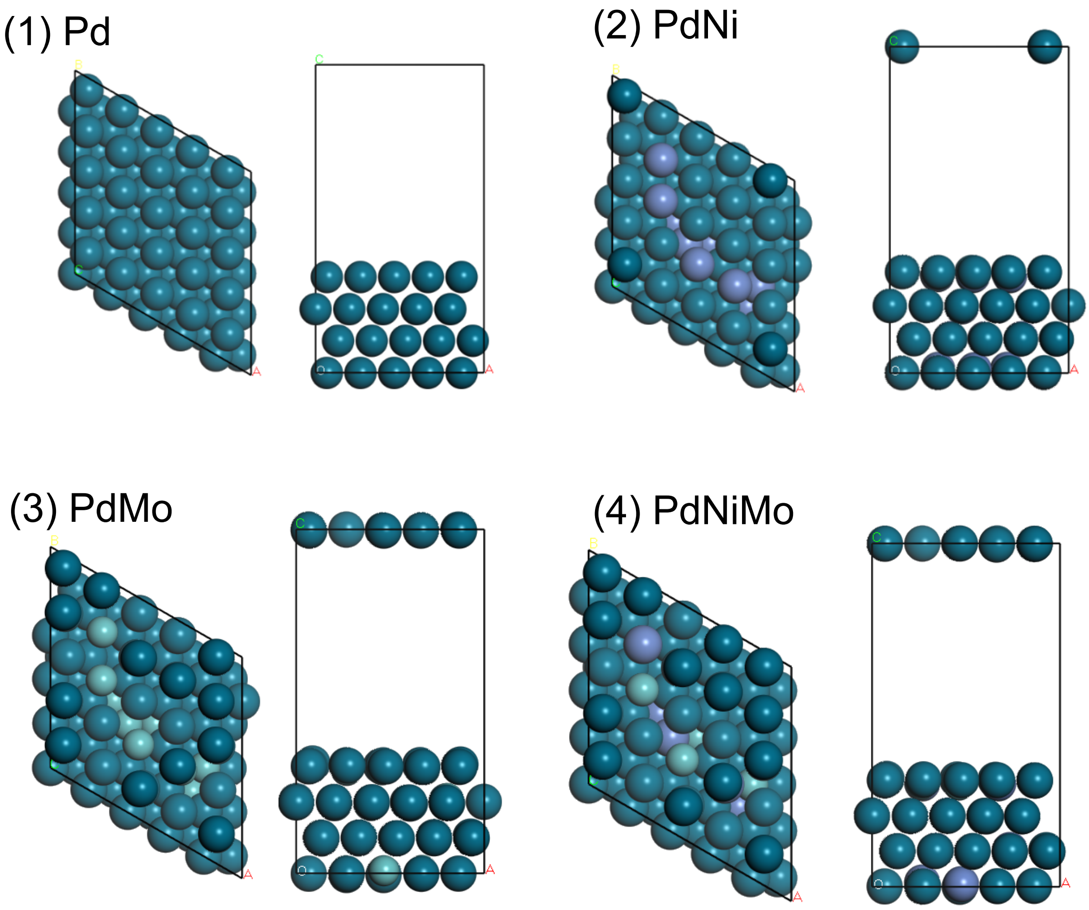

Figure S9. Modeling of Pd-based catalysts

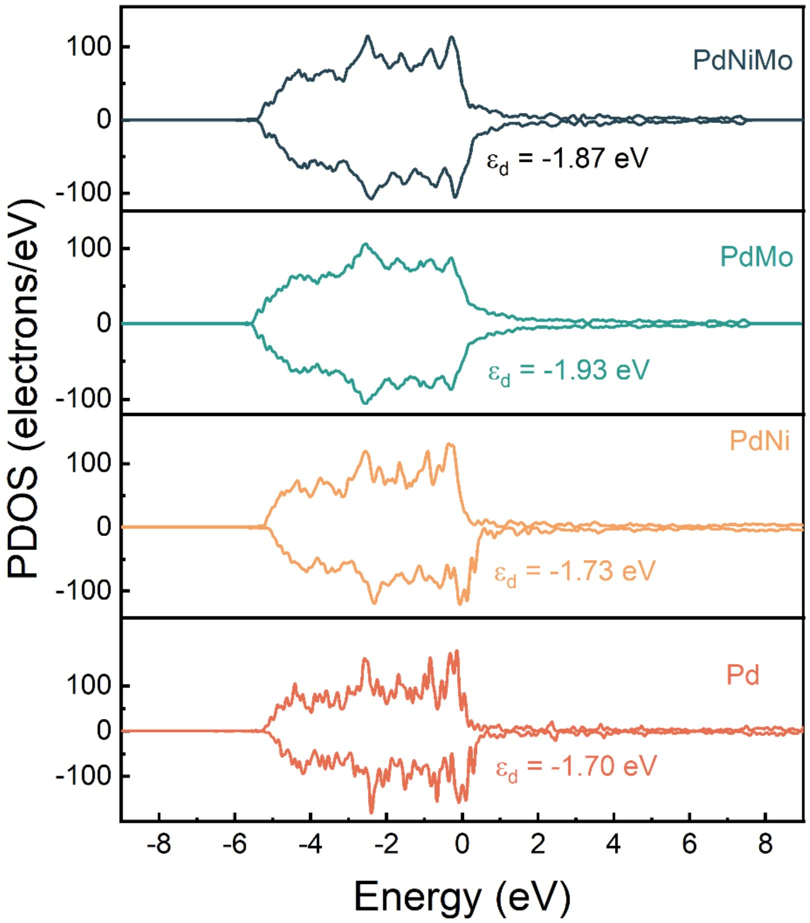

Figure S10. Projected density of states of Pd orbits on PdNiMo, PdMo, PdNi and Pd (111) surface.

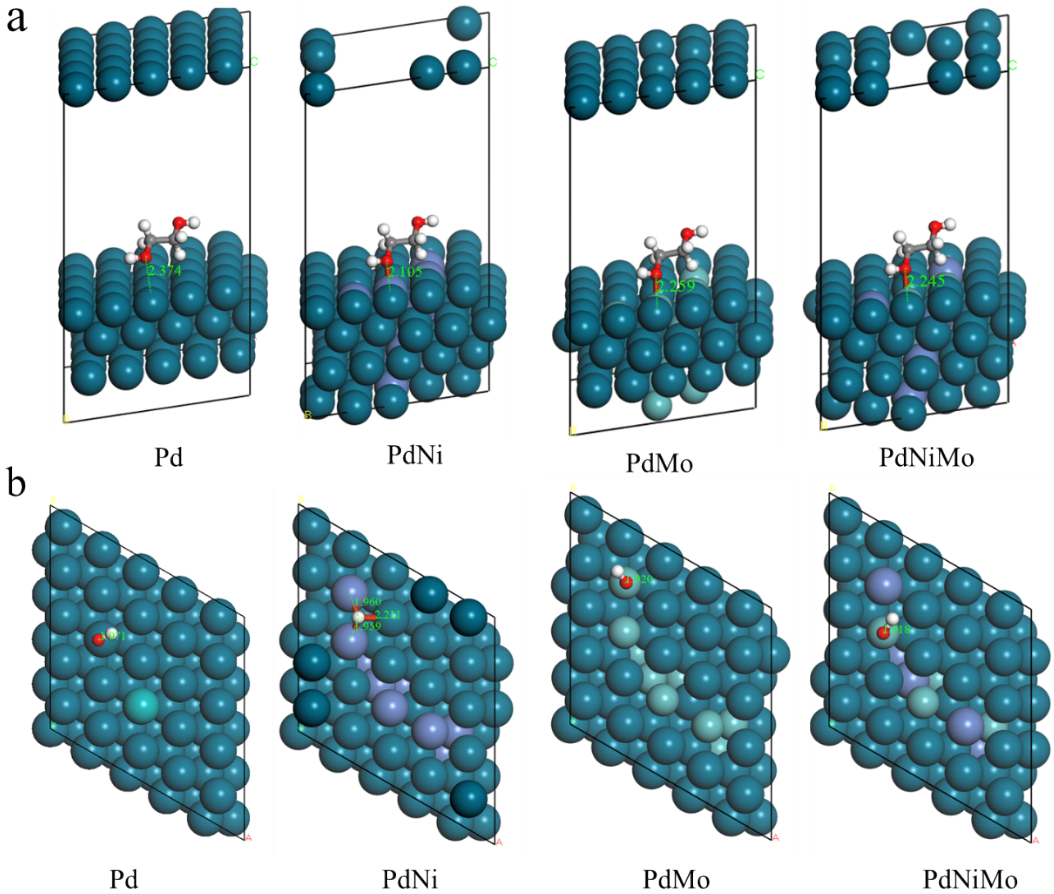

Figure S11. Adsorption structures of a) EG, and b) OH on Pd-based catalysts.

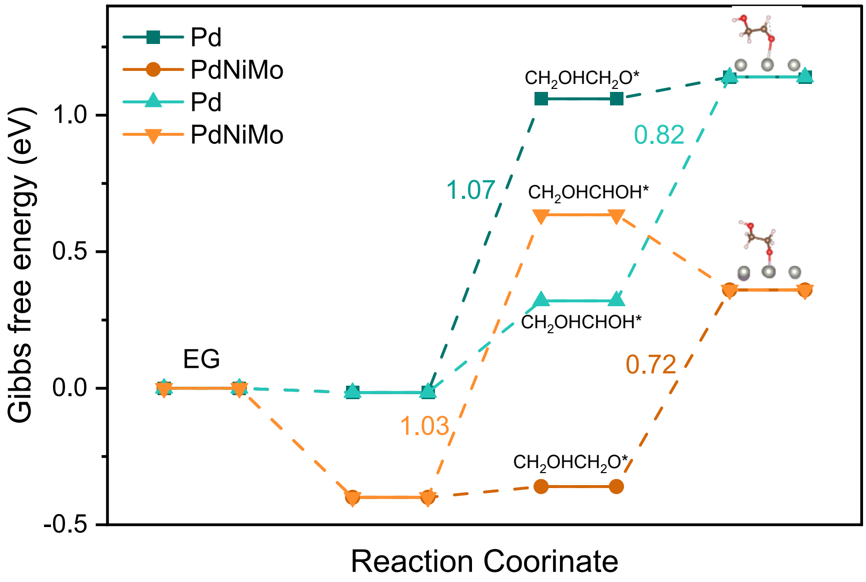

Figure S12. Gibbs free energy diagram and the optimized configurations of EG oxidation to GLYA on Pd and PdNiMo. The colored values are the Gibbs free energy in eV of rate-limiting step.

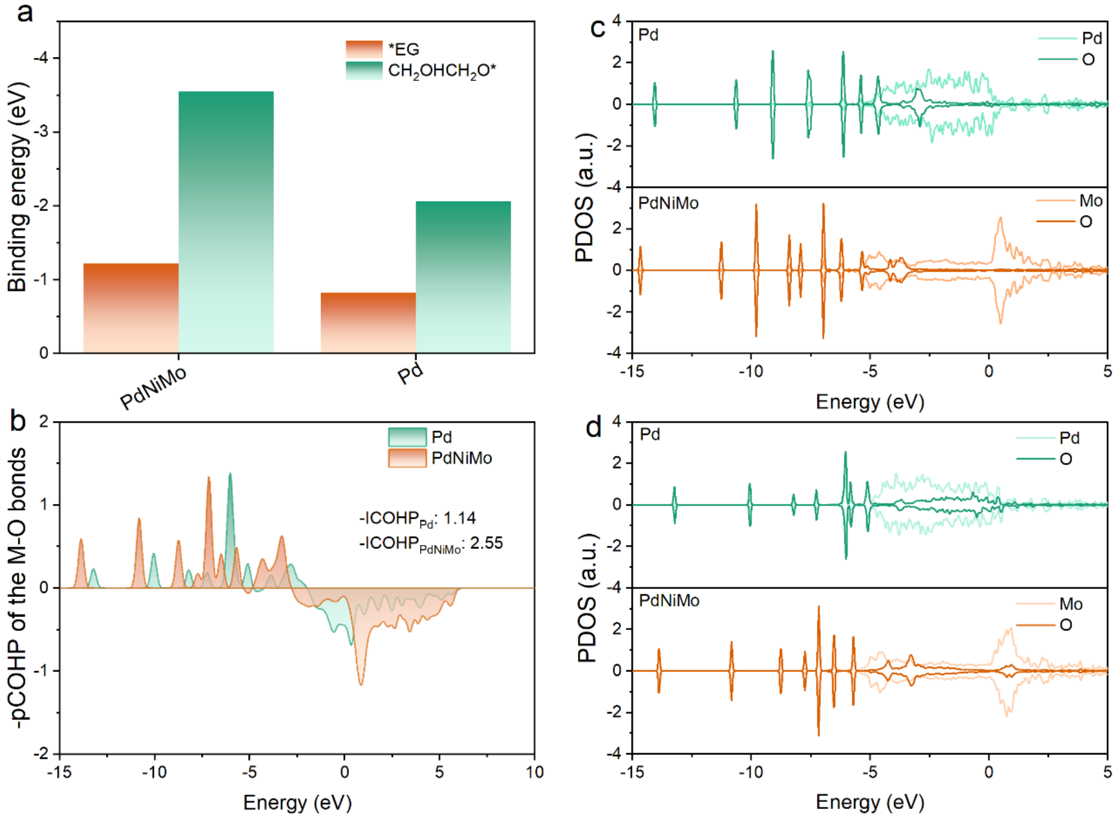

Figure S13. a) Adsorption energies of EG and $*OCH_2CH_2OH$ on Pd and PdNiMo surfaces. b) COHP plots of M-O on different metal surfaces upon adsorption of $*OCH_2CH_2OH$. PDOS diagrams of the M-O bonding of c) EG and d) $*OCH_2CH_2OH$ on different metal surfaces.

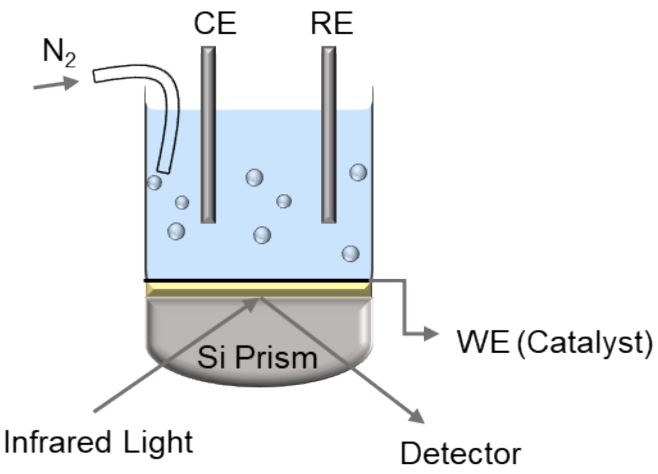

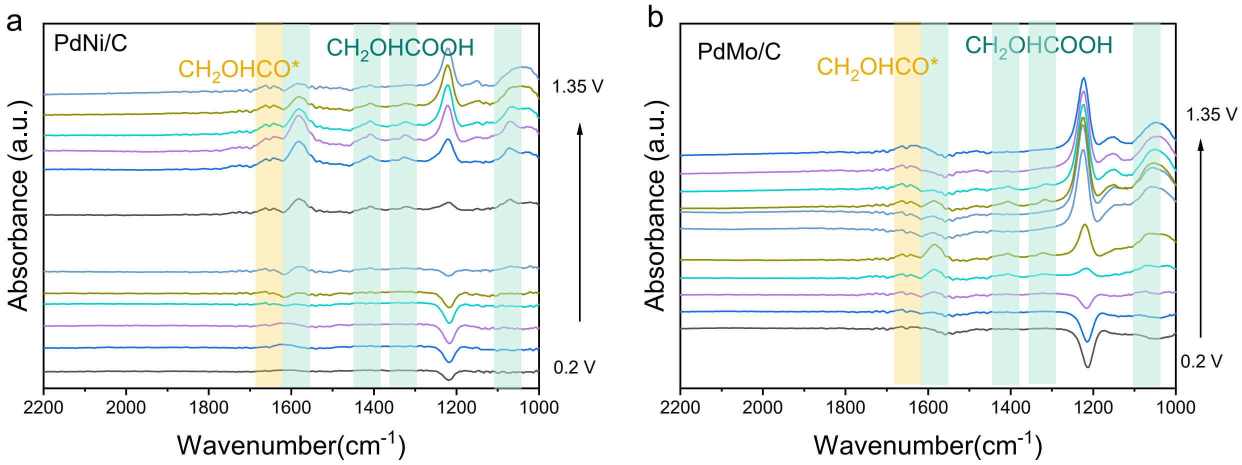

Figure S14. The *in-situ* FTIR spectrum of PdNi/C (a) and PdMo/C (b) in 1.0 M KOH + 1.0 M EG.

Table S1. Summary of vibration bands of the *in-situ* FTIR spectrum.

Wavenumber(cm^{-1})	Functional group or chemical species
1069	ν(C=O) (glyoxal, glycolate)[5, 6]
1220	*S*i-O from the Si prism[7]
1322	ν_s(COO) in glycolate
1409	Typical peak for glycolate or CO_3^{2-}
1581	ν_{as}(COO) in glycolate
1631	ν(C=O) + δ(HOH)[8]
1889	CO_M[9]
2345	CO_2

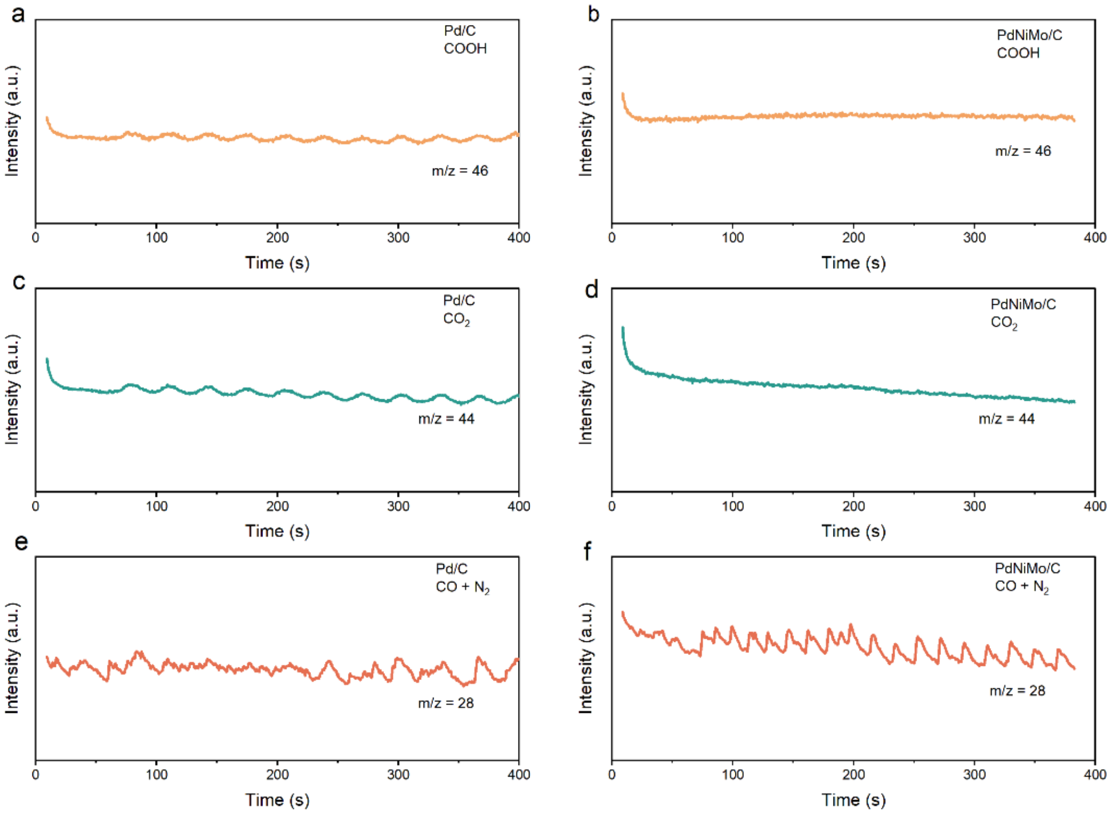

Figure S15. The *in-situ* mass spectrometry of Pd/C (a, c, e) and PdNiMo/C (b, d, f).

Since the *m/z* of both CO and N_2 is 28, it is unable to avoid the interference of N_2 during the detection process. Moreover, the signal of N_2 was significantly stronger than that of CO in the test results, resulting in the inability to determine the presence of CO.

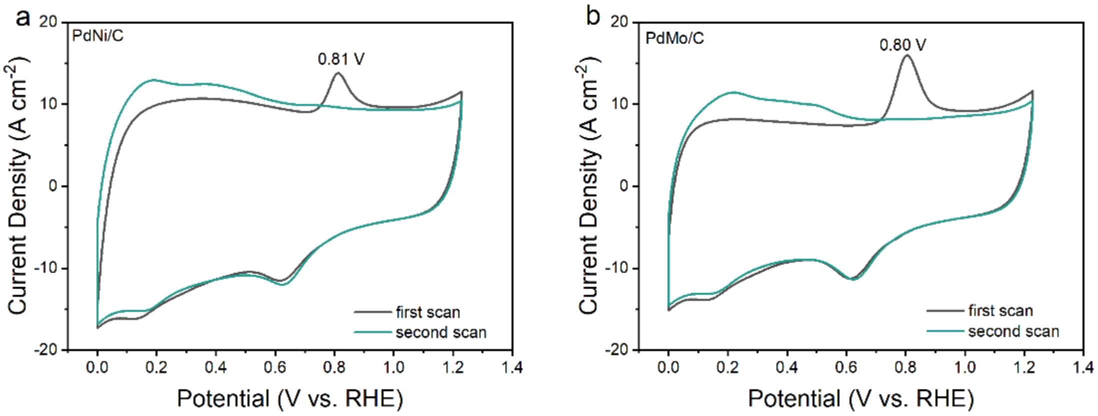

Figure S16. CO stripping of PdNi/C (a) and PdMo/C (b) in 1.0 M KOH with a scan rate of 5 mV/s.

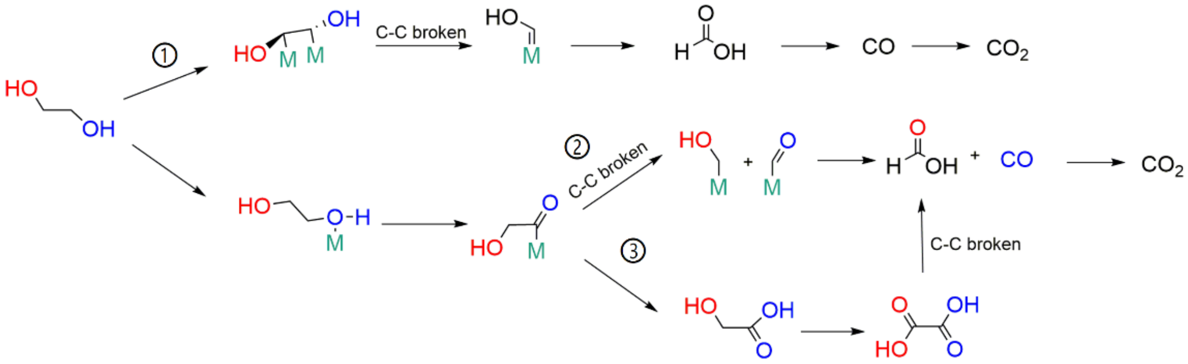

Figure S17. Reaction pathways for C-C bond breaking in the EGOR process.[10-13]

References

1. R. M. Arán-Ais, E. Herrero and J. M. Feliu, *Electrochemistry Communications*, 2014, **45**, 40-43.
2. X.-Y. M. Wei-Yi Zhang1, Shou-Zhong Zou2* , Wen-Bin Cai1*, *JOURNAL OF ELECTROCHEMISTRY*, 2021, **27**, 233-256.
3. T. B. J. K. Nørskov, A. Logadottir, J. R. Kitchin, J. G. Chen,b S. Pandelov, U. Stimming, *Journal ofThe Electrochemical Society*, 2005, **152**, J23-J26.
4. H. J. J. K. NørskovJ. RossmeislA. LogadottirL. LindqvistJ. R. KitchinT. Bligaard, *The Journal of Physical Chemistry B*, 2004, **108**, 17886-17892.
5. W. Z. Yuchen Qin, Fengqi Wang, JunJun Li, Jinyu Ye, Xia Sheng, Chenxi Li, Xiaoyu Liang, Pei Liu, Xiaopeng Wang, Xin Zheng, Yunlai Ren, Cuilian Xu,* and Zhicheng Zhang*, *Angew. Chem. Int. Ed.*, 2022, **61**, e202200899.
6. R. G. Da Silva, A. Rodrigues de Andrade, K. Servat, C. Morais, T. W. Napporn and K. B. Kokoh, *ChemElectroChem*, 2020, **7**, 4326-4335.
7. a. T. N. Dominik Enders, *a Annemarie Pucci,b Tomonobu Nakayamaa and Masakazu Aonoa, *Phys. Chem. Chem. Phys*, 2011, **13**, 4935–4941.
8. Y. Qi, Y. Zhang, L. Yang, Y. Zhao, Y. Zhu, H. Jiang and C. Li, *Nature Communications*, 2022, **13**.
9. W. Huang, X. Y. Ma, H. Wang, R. Feng, J. Zhou, P. N. Duchesne, P. Zhang, F. Chen, N. Han, F. Zhao, J. Zhou, W. B. Cai and Y. Li, *Advanced Materials*, 2017, **29**.
10. F. Liu, X. Gao, R. Shi, Z. Guo, E. C. M. Tse and Y. Chen, *Angewandte Chemie International Edition*, 2023, **62**.
11. J. Li, L. Li, X. Ma, X. Han, C. Xing, X. Qi, R. He, J. Arbiol, H. Pan, J. Zhao, J. Deng, Y. Zhang, Y. Yang and A. Cabot, *Advanced Science*, 2023, **10**.
12. W. Chen, J. Shi, C. Xie, W. Zhou, L. Xu, Y. Li, Y. Wu, B. Wu, Y.-C. Huang, B. Zhou, M. Yang, J. Liu, C.-L. Dong, T. Wang, Y. Zou and S. Wang, *National Science Review*, 2023, **10**.
13. W. Chen, J. Shi, Y. Wu, Y. Jiang, Y. C. Huang, W. Zhou, J. Liu, C. L. Dong, Y. Zou and S. Wang, *Angewandte Chemie International Edition*, 2023, **63**.